Journal of Alloys and Compounds 509 (2011) 9240–9245

Contents lists available at ScienceDirect

Journal of Alloys and Compounds

journal homepage: www.elsevier.com/locate/jallcom

Metallic inorganic/organic hybrid system through functionalized Schiff-base linkage: Molecular assembly, characterization and luminescence

Bing Yan*, Jun-Wei Wang, Ya-Juan Li

Department of Chemistry, Tongji University, Siping Road 1239, Shanghai 200092, China

ARTICLE INFO

Article history:
Received 9 May 2011
Received in revised form 5 July 2011
Accepted 5 July 2011
Available online 12 July 2011

Keywords:
Schiff base linkage
Metallic organic/inorganic hybrids
Mesoporous hybrids
Luminescence

ABSTRACT

In this paper, two Schiff-base compounds (N,N′-bis(salicylidene)-1,3-ethylenediamine (BSEA) and N,N′N″-tris(salicylidene)-(2-aminoethyl) amine (TSAEA)) are modified with a crosslinking reagent isocyanate propyl triethoxysilane (TESPIC) to achieve two linkages (BSEASi and TSAEASi). Then metallic (Ni^{2+}, Mn^{2+}, Co^{2+}) inorganic/organic hybrids with functionalized Schiff-base linkages are prepared with coordination bonding. Then the corresponding mesoporous hybrids with BSEASi functionalized SBA15 host are assembled. All these hybrids are characterized in detail and particularly the photoluminescence of them shows that they all show the luminescence of the organically bonded host and metal ions that only disturb it.

1. Introduction

Inorganic/organic hybrid materials have been subjected to the dramatic development in the field of materials science since they not only combine the respective beneficial characters of organic and inorganic components, but also often exhibit unique properties that exceed what would be expected for a simple mixture of the components [1,2]. Among the most important types are so-called the chemically bonded hybrids through the integration of chemical bonding within the different units in a complicated system, which can realize the possibility of tailoring the complementary properties of both components to obtain novel multifunctional materials with attractive behaviors, such as mechanical, thermal and other physical and chemical properties [3,4].

Among the silica-based hybrids organically modified polysilsesquioxane as a linkage is mainly studied in the field of organic–inorganic hybrid materials through the sol–gel technology between different silicon alkoxides [5–7]. Carlos et al. have done an important work and lately given a review on the lanthanide-containing light-emitting organic–inorganic hybrids [8–10]. More recently, Binnemans gives a more extensive overview of the different types of lanthanide-based hybrid materials and compared their respective advantages and disadvantages [11]. Our research team is presently engaged in the extensive work and we concentrate on covalently grafting the ligands to the inorganic networks in which lanthanide complexes luminescent centers, which are bonded with a siloxane matrix through Si–O linkage and we have successfully realized six paths to construct the functional silylated precursors. In addition, after the modification, we assembled the above modified bridge ligands with lanthanide ions and tetraethoxysilane (TEOS) to compose hybrid systems with covalent bonds and obtained series of stable and efficient molecular hybrid materials in optical areas [12–18].

Further, the organic–inorganic mesoporous hybrids through the modification of mesoporous host have been paid attention for their advantages: firstly, the organic groups can be dispersed in the pore or in the surface and cannot traffic the pore channel; secondly, organic groups can provide the whole materials systems with some new functions such as the electronics, optics, and magnetic. These advantages will embody the hybrid with flexible modification of physical and chemical properties, which can be expected to develop some new practical application. So lately, a lot of work has been shifted to the preparation of mesoporous hybrids [19–24].

Schiff-base derivatives belong to the compounds with double bonds between nitrogen and carbon atoms, which can exhibit various properties to be applied to such fields as organic synthesis, catalyst, liquid crystal and bioinorganic chemistry [25–27]. In term of the superior flexibility of them in the synthesis and modification, Schiff-base can be introduced in the inorganic/organic hybrid materials systems through the coordination of the electron in their N or C atoms to metal ion. This not only can form chelates with metal ions but also can enhance the functionality of organic groups. Most of the Schiff-base ligands are synthesized from the salicylidene or its derivative with diamine. Few reports on materials having Schiff-base derivatives covalent with the silica network and their photoluminescence properties have been reported [28,29]. We

* Corresponding author. Tel.: +86 21 65984663; fax: +86 21 65982287.
E-mail address: byan@tongji.edu.cn (B. Yan).

0925-8388/$ – see front matter © 2011 Elsevier B.V. All rights reserved.
doi:10.1016/j.jallcom.2011.07.006

have synthesized series of Schiff-base modified silica hybrids and fatherly prepared the mesoporous hybrids [30,31], which can possess interesting blue or blue-green luminescence in visible region.

In this paper, on the basis of our previous work, we introduce the metal ions in the hybrid systems through the coordination bonding and prepared six kinds of metallic (Ni^{2+}, Mn^{2+}, Co^{2+}) centered hybrids with two Schiff-base modified covalent linkages and then assembled the corresponding mesoporous hybrids with SBA-15 host. The detailed characterization and luminescence are reported.

2. Experimental

2.1. Starting materials and chemicals

Pluronic P123 ($EO_{20}PO_{70}EO_{20}$, Aldrich), 3-(triethoxysiyl)-propyl isocyanate (TESPIC, Lancaster), and tetraethoxysilane (TEOS, Aldrich) are distilled and stored under nitrogen atmosphere. All the other reagents are analytically pure and from Shanghai Chemical Plant. The solvents are purified according to the literature procedures [32].

2.2. The synthesis of Schiff base compounds, the functionalized precursors

The di-Schiff base compound N,N′-bis(salicylidene)-1,3-ethylenediamine (BSEA) and tri-Schiff base compound N,N′N″-tris(salicylidene)-(2-aminoethyl) amine (TSAEA) and the silylated precursors (BSEASi, TSAEASi) are prepared according to the procedure depicted in Refs. [29–31]. BSEA: 85%. TSAEA: yields 76%. ^{1}H NMR ($CDC1_3$): δ 2.70 (t, 6H, NCH_2); 3.67 (t, 6H, CH_2N=*CH*); 6.85, 6.94, 7.24, 7.30 (12H, Ar); 8.40 (s, 3H, *Ar*CH); 13.02 (s, 3H, OH). TSAEASi: yields 68%. ^{1}H NMR ($CDC1_3$): δ 0.60 (t, 6H, CH_2Si); 1.22 (t, 27H, CH_3CH_2); 1.60 (m, 6H, $NHCH_2CH_2CH_2Si$); 2.70 (t, 6H, NCH_2); 3.17 (m, 6H, $NHCH_2$); 3.60 (q, 18H, $SiOCH_2$); 3.67 (t, 6H, CH_2N=*CH*); 6.85, 6.92, 7.25, 7.32 (12H, Ar); 8.01 (t, 3H, NH); 8.41 (s, 3H, *Ar*CH) [1].

2.3. The synthesis of the metallic covalently bonded hybrids

The precursor (BSEASi, TSAEASi, 1 mmol) is dissolved in DMF (20 mL), and suitable amount of metal salts, TEOS, and H_2O are added. The molar ratio of precursor/TEOS/H_2O is 1:(2)2:6. And then one drop of diluted hydrochloric acid is added to promote hydrolysis reaction. After 2 h, a small amount of hexamethylenetetramine (0.05 g) is added to stimulate the polycondensation reaction. The resulting solution is vigorously stirred for 4 h. The resulting sol is aged in covered Teflon beakers at room temperature until the onset of gelation, after that thermal treatment is performed at 60 °C until the sample solidified. The powder materials are then obtained after being washed with ethanol and dried for 2 days (see Fig. 1A).

2.4. Synthesis of metallic Schiff-base functionalized SBA-15 mesoporous hybrids

SBA-15 host structure is synthesized according to the reported procedure using Pluronic P123 as a structure-directing agent and tetraethyl orthosilicate (TEOS) as a silica source under acidic conditions [33,34]. And then the mesoporous materials M-BSEA-SBA-15 and (M = Ni, Co, Mn) are synthesized from acidic mixture with the following molar composition: 0.0172 P123:0.83 TEOS:0.17 BSEA-Si:6 HCl:208.33 H_2O. P123 (1.0 g) is dissolved in the deionized water (7.5 g) and 2 M HCl solution (30 g) at room temperature. A mixture of BSEASi and TEOS is added into the above solution with stirring for 24 h and transferred into a Teflon bottle sealed in an autoclave, which is heated at 100 °C for 48 h. The solid product is filtered, washed thoroughly with deionized water, and dried at 65 °C. Removal of copolymer surfactant P123 is conducted by Soxhlet extraction with ethanol under reflux for 2 days. The material is dried in a vacuum and shows light-yellow color (Fig. 1B).

2.5. Physical characterization

^{1}H NMR spectra were recorded on a BRUKER AVANCE-500 spectrometer with tetramethylsilane (TMS) as internal reference using $CDCl_3$ as solvent. IR spectra were measured within the 4000–400 cm^{-1} region on an infrared spectrophotometer with the KBr pellet technique. The Ultraviolet absorption spectra were taken with an Agilent 8453 spectrophotometer (CCl_4 solution). X-ray powder diffraction patterns were recorded on a Rigaku D/max-rB diffractometer equipped with a Cu anode in a 2θ range from 0.6 to 6° Nitrogen adsorption/desorption isotherms were measured at the liquid nitrogen temperature, using a Nova 1000 analyzer. Before the measurements, the samples were outgassed for 2 h in the degas port of the adsorption apparatus at 423 K. Surface areas were calculated by the Brunauer–Emmett–Teller (BET) method and pore size distributions were evaluated from the desorption branches of the nitrogen isotherms using the Barrett–Joyner–Halenda (BJH) model. Thermogravimetric analysis (TGA) is performed on a Netzsch STA 409 at a heating rate of 15 °C/min under nitrogen atmosphere. The fluorescence excitation and emission spectra were obtained on RF-5301 spectrophotometer. All spectra are normalized to a constant intensity at the maximum.

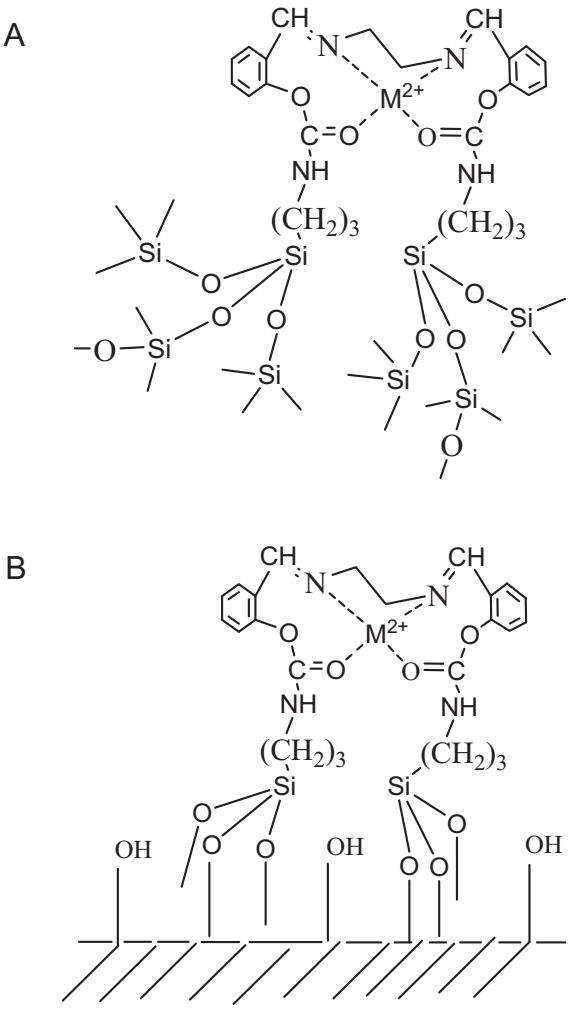

Fig. 1. The scheme for the chemically bonded hybrids M-BSEA-Si (M = Ni, Co, Mn) (A) and mesoporous hybrids M-BSEA-SBA-15 (M = Ni, Co, Mn) (B).

3. Results and discussion

Fig. 2A shows the FT-IR spectra of selected metallic chemically bonded hybrids Ni-BSEA-Si and Co-BSEA-Si, both of which show the similar feature. The main absorption peaks of Schiff-base all can be found in the IR spectra of hybrids. There are three absorption peak at 1080 cm^{-1} (ν_{as}, Si–O), 800 cm^{-1} (ν_s, Si–O) and 450 cm^{-1} (δ, Si–O–Si), suggesting that the formation of Si–O–Si network within the hybrid system. In addition, the appearance of 1650 cm^{-1} and 1500 cm^{-1} is due to the amide group (–CONH–) of BSEASi. The wide band at around 3000 cm^{-1} and 3400 cm^{-1} corresponds to the hydroxyl groups of association, which derives from the H_2O molecules or incompletely hydrolysis of Si–OH group in the sol–gel process. In addition, the bands at the range of 2850–3000 cm^{-1} to the vibrations of methylene $-(CH_2)_3-$ are present and the stretch vibration of the absorption peaks at 2250–2275 cm^{-1} for N=C=O of TESPIC disappear, revealing the modification of TESPIC by Schiff-base compounds. In the low frequency regions, the apparent peak corresponding to the M–O coordination bonds can be observed at around 470 cm^{-1}. Fig. 2B presents the FT-IR spectra of the three metallic mesoporous hybrids. The apparent characteristic absorption peaks of amino groups cannot be observed at the high frequency except for the wide absorption bands ascribed to the H_2O molecule within the hybrid system. In addition, the amide reactions of TESPIC with Schiff-base are verified by the bands located at around 1600 cm^{-1} of the vibration absorption and 1500 cm^{-1} of the

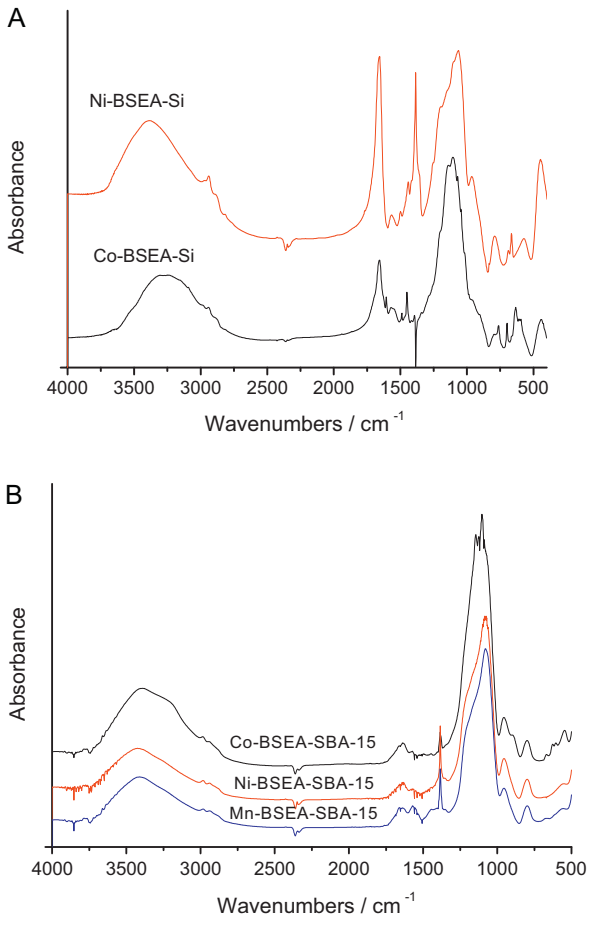

Fig. 2. The FT-IR spectra of BSEASi bridge, hybrids BSEA-Si-Ni and BSEA-Si-Co (A) and mesoporous hybrids M-BSEA-SBA-15 (M = Ni, Co, Mn) (B).

bending vibration of amide groups (–CONH–). Besides, the bands at the range of 2850–3000 cm^{-1} to the vibrations of methylene $-(CH_2)_3-$ are present and the stretch vibration of the absorption peaks at 2250–2275 cm^{-1} for N=C=O of TESPIC disappear, revealing the modification of TESPIC by Schiff-base compounds. The absorption bands at 460, 800 and 1080 cm^{-1} are ascribed as the asymmetry, symmetry stretching vibration and plane bending vibration, respectively, suggesting that the formation of Si–O–Si network structure in the mesoporous systems.

Fig. 3 shows the XRD patterns of metallic chemically bonded hybrids through Schiff-base linkage. Thus, the presence of diffraction peaks can be used to evaluate the structural order at long range or periodicity of the material [35]. The wide diffractograms without apparent sharp peak of these patterns show that all the hybrids are amorphous or non-periodic. The broad peak centered around 22° in the XRD patterns may be ascribed to the coherent diffraction of the siliceous backbone of the hybrids [36]. The organic complex which was covalently linked into silica matrixes by the strong Si–C bonds did not change the overall disorder structure of the siliceous skeleton. The formation of the true covalent-bonded molecular hybrid materials can be proved by the fact that none of the hybrid materials contains measurable amounts of phases corresponding to the pure organic compound. No diffraction of ligands and metal salts can be found in the curves, which suggests that these hybrids belong to the complicated system to molecular degree and not simple physically doping. The small-angle X-ray diffraction (SAXRD) patterns are popular and efficient method to characterize highly ordered mesoporous material with hexagonal symmetry of the space group *p6mm*. The SAXRD patterns of pure

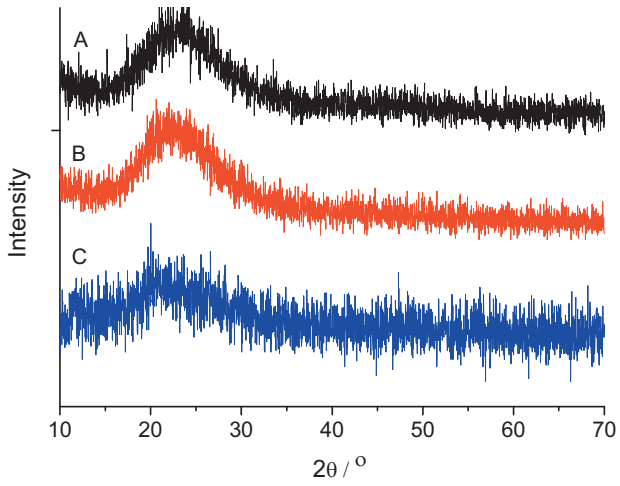

Fig. 3. The XRD patterns of hybrids Ni-BSEA (A), Mn-BSEA (B) and Co-BSEA (C).

SBA-15 mesoporous silica, Ni-BSEA-SBA-15, Co-BSEA-SBA-15 and Mn-BSEA-SBA-15 are presented in Fig. 4. All the materials exhibit three well-resolved diffraction peaks at the range of 0.8–2.0° that can be indexed as (1 0 0), (1 1 0), and (2 0 0) reflections associated with 2-D hexagonal symmetry (*p6mm*), confirming a well-ordered mesoporous structure in these samples. Compared with the SAXRD pattern of pure SBA-15, the d_{100} spacing values of M-BSEA-SBA-15 are hardly changed (see Table 1) except for the slight decrease of diffraction intensity, indicating that the ordered hexagonal mesoporous structure of SBA-15 retains intact after the introduction of organic group and the presence of guest moieties onto the mesoporous framework of SBA-15 produce the decrease of crystallinity [20].

The selected scanning electron micrographs of the chemically bonded hybrids are shown in Fig. 5 (A for Ni-BSEA-Si, B for Co-BESA-Si and C for Mn-BSEA-Si). The uniform frameworks on the surface of all the hybrid materials demonstrate that homogeneous systems containing covalent bonds between the organically modified group (BSEASi) and inorganic matrices, and coordination bonds between BSEASi and metal ions are obtained. It can be found that no phase separation appears in these hybrid materials and the inorganic and organic phases in the hybrids can exhibit their distinct properties together. Further, both of them exhibit many dendritic stripe microstructure, which is dispersed regularly on the surface of the hybrid material. New small branches emerge at the end of each

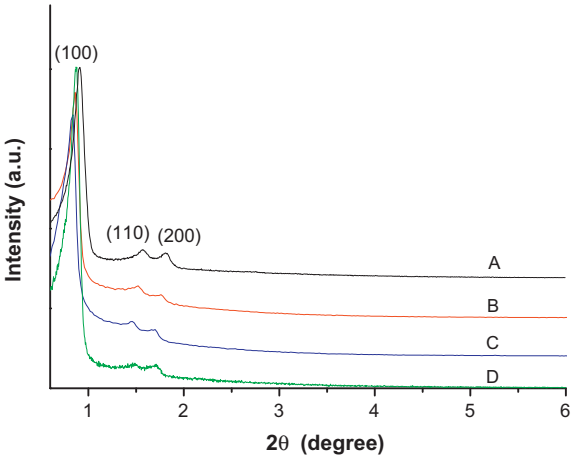

Fig. 4. Small angle X-rays diffraction patterns of mesoporous hybrids SBA-15 (A), Ni-BSEA-SBA-15 (B), Mn-BSEA-SBA-15 (C) and Co-BSEA-SBA-15 (D).

Table 1
The structural data of mesoporous hybrids of SBA-15, Ni-BSEA-SBA-15, Co-BSEA-SBA-15 and Mn-BSEA-SBA-15.

Sample	d (nm)	a_0 (nm)	S_{BET} (m^2/g)	V (cm^3/g)	D_{BJH} (nm)	t (nm)
SBA-15	10.26	11.85	752	1.02	6.02	5.83
Ni-BSEA-SBA-15	10.51	12.14	511	0.94	5.95	6.19
Mn-BSEA-SBA-15	10.15	11.72	480	0.91	5.91	5.81
Co-BSEA-SBA-15	9.81	11.33	439	0.77	5.51	5.82

d_{100} is the $d(1\,0\,0)$ spacing, a_0 the cell parameter ($a_0 = 2d_{100}/\sqrt{3}$), S_{BET} the BET surface area, V the total pore volume, D_{BJH} the average pore diameter, and t the wall thickness, calculated by $a_0 - D$.

dendritic stripe, and the stripes will continue to grow according to the direction of these branches to form the final structure. With the introduction of metal ions, the coordination reaction between metal ions and BSEASi will compete with the cohydrolysis and copolycondensation reaction in the formation of the whole hybrid material system. So the coordination interaction will have influence on the construction of the three-dimensional Si–O–Si network structure in the hydrolysis and polycondensation process. In conclusion, the microstructure of the hybrid materials depends on many factors, and both organic ligands and rare ions can largely influence the self-assemble process of the hybrids.

Fig. 6 presents the N_2 adsorption–desorption isotherm (top plot) and the pore size distribution (bottom plot) for pure SBA-15, Ni-BSEA-SBA-15, Mn-BSEA-SBA-15 and Co-BSEA-SBA-15 mesoporous materials. They all show Type IV isotherms with H1-type hysteresis loops at high relative pressure according to the IUPAC classification [37,38], which belongs to the typical character of mesoporous materials with highly uniform size distributions. From the two branches of adsorption–desorption isotherms, the presence of a sharp adsorption step in the P/P_0 region from 0.6 to 0.8 and a hysteresis loop at the relative pressure $P/P_0 > 0.7$ show that the materials process a well defined array of regular mesopores. The specific area and the pore size have been calculated by using Brunauer–Emmett–Teller (BET) and Barrett–Joyner–Halenda (BJH) methods, respectively, whose structure data of all these mesoporous materials (BET surface area, total pore volume, pore size, etc.) are summarized in Table 1. It is known that calcined SBA-15 has a high BET surface area (752 m^2/g), a large pore volume (1.02 cm^3/g) and pore size (5.83 nm), indicative of its potential application as a host in luminescence materials. After functionalized with BSEA through covalent bond, the M-BSEA-SBA-15 mesoporous hybrids exhibit a smaller specific area and a slightly smaller pore size and pore volume in comparison with those of pure SBA-15, which might be due to the presence of organic BSEA group on the pore surface and the co-surfactant effect of BSEASi, which interacts with surfactant and reduces the diameter of the micelles [39].

Fig. 7A and B shows the excitation and emission spectra of the covalently bonded hybrid materials Ni-BSEA-Si, Co-BSEA-Si and Mn-BSEA-Si. From the excitation spectra, both Ni-BSEA-Si and

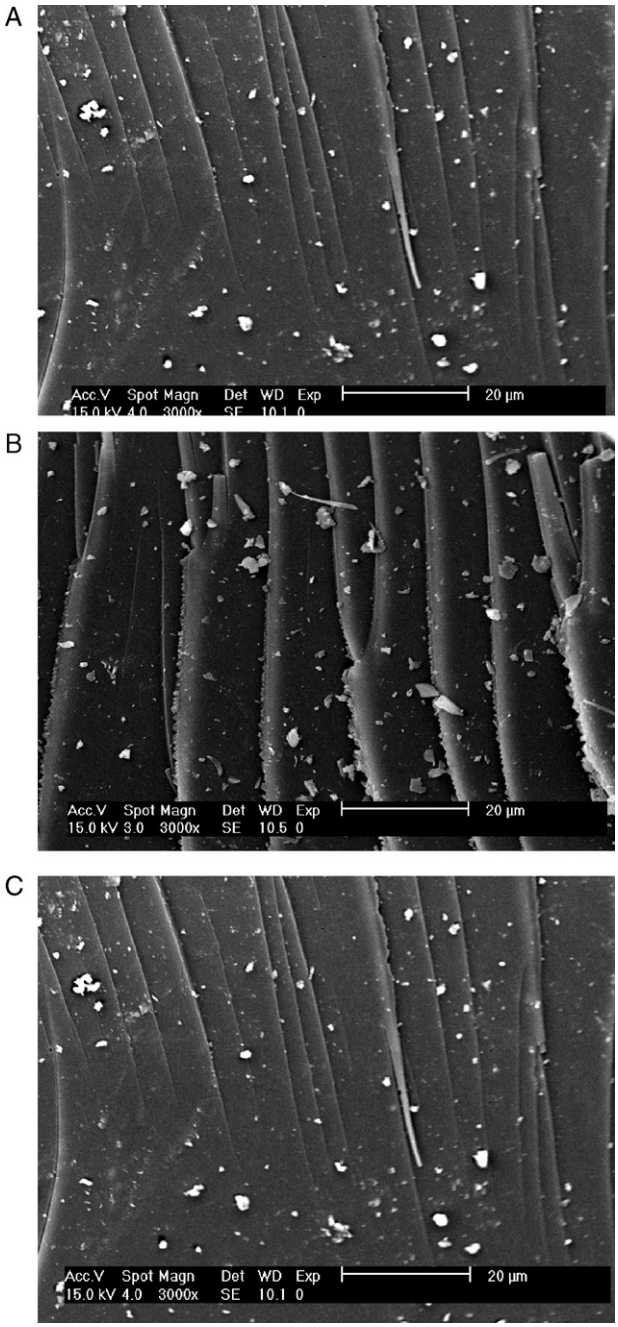

Fig. 5. The SEM images of selected hybrids Ni-BSEA-Si (A), Co-BSEA-Si (B) and Mn-BSEA-Si (C).

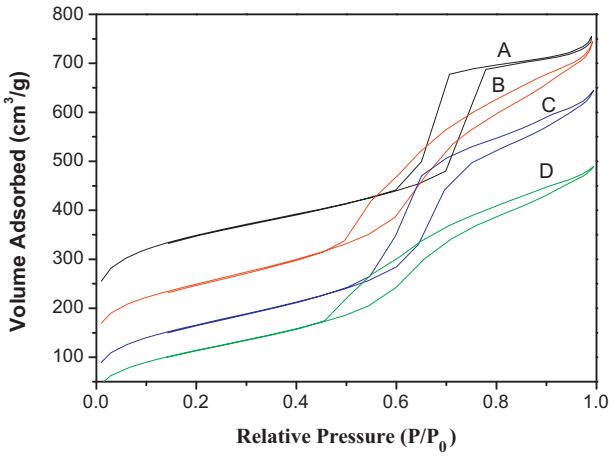

Fig. 6. The N_2 adsorption–desorption curves of mesoporous hybrids SBA-15 (A), Ni-BSEA-SBA-15 (B), Mn-BSEA-SBA-15 (C) and Co-BSEA-SBA-15 (D).

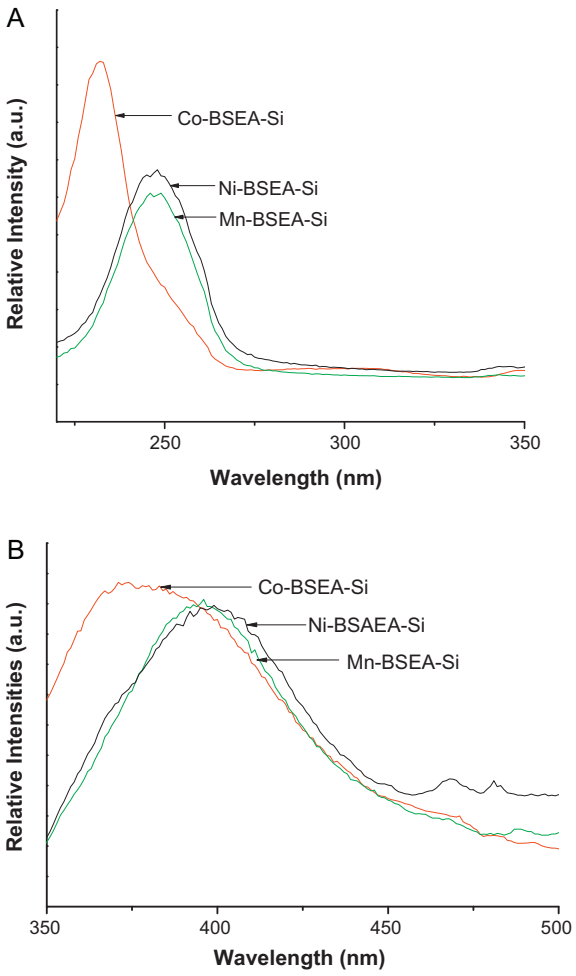

Fig. 7. Luminescent excitation (A) and emission (B) spectra of hybrids Ni-BSEA-Si, Co-BSEA-Si and Ni-TSAEA-Si.

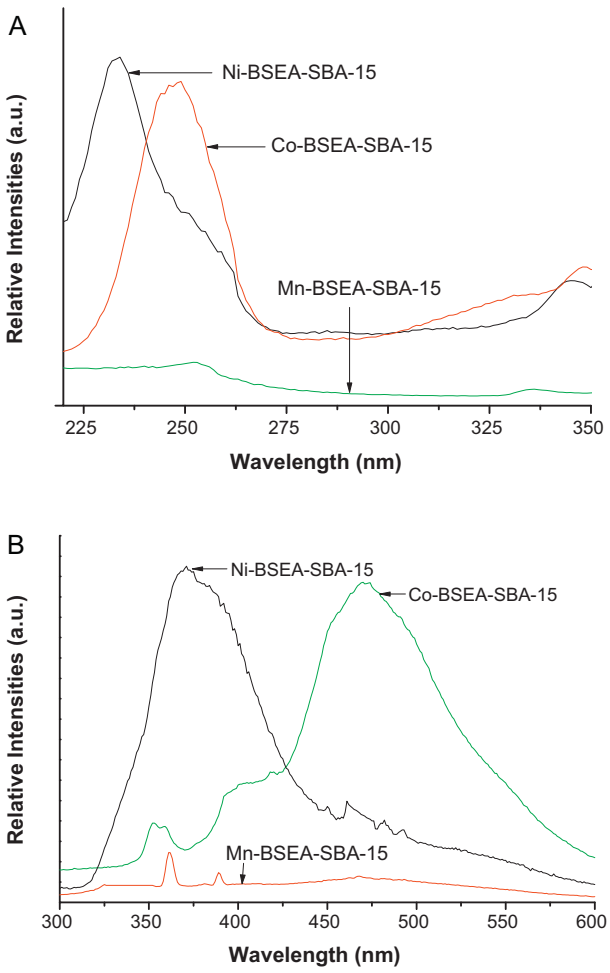

Fig. 8. Luminescent excitation (A) and emission (B) spectra of mesoporous hybrids Ni-BSEA-SBA-15, Co-BSEA-SBA-15, Mn-BSEA-SBA-15.

Mn-BSEA-Si hybrids show the similar maximum excitation peak of around 250 nm while it is at 230 nm for Co-BSEA-Si hybrids. This indicates that the different transition metal ions have apparent influence on the energy absorption of the complex system through the coordination interaction between them and the C=O of the organically BSEASi group. Subsequently, the corresponding emission spectra of the three covalently bonded hybrids show different bands in the ultraviolet–visible region, which is similar to the excitation spectra. Both Ni^{2+} and Mn^{2+} hybrids present the maximum emission peaks at around 400 nm, while Co^{2+} hybrid system exhibits the peak of 350 nm. As the d orbital is sensitive to the ligands and the three transition metal ions have strong coordination interaction with the C=O group of BSEASi, so the luminescence of the whole hybrid system is affected obviously.

For the mesoporous hybrids, the luminescence behavior has also shown the differences compared to that of the above hybrid one (Fig. 8). For the excitation spectra in Fig. 8A, Co-BSEA-SBA-15 hybrids show the maximum excitation peak at 235 nm while Ni-BSEA-SBA-15 and Mn-BSEA-SBA-15 hybrids show the ref-shift of maximum excitation peak at 245 nm. For the same BSEA functionalized SBA-15, different transition metal ions still affect energy absorption of the whole hybrid system through the coordination bond of M–O=C, which is not generally corresponded to the results of covalently bonded hybrids without mesoporous host. This suggests that the strong coordination effect of transition metal ions complex system has large and complicated influence on the luminescence behavior of the whole system, which is difficult to predict clearly. Different from the non-mesoporous hybrids, the emission spectra of the three mesoporous hybrids show different bands in the ultraviolet–visible region, which is similar to the excitation spectra. Both Ni^{2+} and Mn^{2+} hybrids present the maximum emission peaks at around 400 nm, while Co^{2+} hybrid system exhibits the peak of 350 nm. As the d orbital is sensitive to the ligands and the three transition metal ions have strong coordination interaction with the C=O group of BSEASi, so the luminescence of the whole hybrid system is affected obviously. As well the emission spectra show different phenomena, both Co and Mn mesoporous hybrids possess the blue emission centered in 470 nm, while Ni system presents the ultraviolet light at 370 nm. The big distinction between them cannot be understood exactly.

4. Conclusions

To sum up, some metal ions (Ni^{2+}, Co^{2+}, Mn^{2+}) organic–inorganic hybrid materials have been prepared through the functionalized Schiff-base linkage and the corresponding mesoporous hybrids are also assembled with SBA-15 host. All these hybrids are characterized and especially the luminescence properties of them are investigated, suggesting that the metal–O coordination bond has an apparent influence on the excitation and emission of the whole hybrid system.

References

[1] E.J. Nassar, O.A. Serra, I.L.V. Rosa, J. Alloys Compd. 250 (1997) 380–382.
[2] P.G. Romero, Adv. Mater. 13 (2001) 163–174.
[3] M. Schneider, K. Muller, Chem. Mater. 12 (2000) 352–362.
[4] F.Y. Liu, L.S. Fu, H.J. Zhang, New J. Chem. 27 (2003) 233–235.
[5] K.J. Shea, D.A. Loy, Chem. Mater. 13 (2001) 3306–3319.
[6] R.J.P. Corriu, D. Leclercq, Angew. Chem. Int. Ed. Engl. 35 (1996) 1420–1436.
[7] R.J.P. Corriu, Angew. Chem. Int. Ed. 39 (2000) 1376–1398.
[8] R.A.S. Ferreira, L.D. Carlos, R.R. Goncaülves, S.J.L. Ribeiro, V.D. Bermudez, Chem. Mater. 13 (2001) 2991–2998.
[9] M.C. Goncalves, V.D. Bermudez, R.A.S. Ferreira, L.D. Carlos, D. Ostrovskii, J. Rocha, Chem. Mater. 16 (2004) 2530–2543.
[10] L.D. Carlos, R.A.S. Ferreira, V.D. Bermudez, S.J.L. Ribeiro, Adv. Mater. 21 (2009) 509–534.
[11] K. Binnemans, Chem. Rev. 109 (2009) 4283–4374.
[12] Q.M. Wang, B. Yan, J. Mater. Chem. 14 (2004) 2450–2454.
[13] B. Yan, Y.L. Sui, J.L. Liu, J. Alloys Compd. 476 (2009) 826–829.
[14] J.L. Liu, B. Yan, J. Phys. Chem. B 112 (2008) 10898–10907.
[15] H.F. Lu, B. Yan, J.L. Liu, Inorg. Chem. 48 (2009) 3966–3975.
[16] B. Yan, Q.M. Wang, Cryst. Growth Des. 6 (2008) 1484–1489.
[17] B. Yan, H.F. Lu, Inorg. Chem. 47 (2008) 5601–5611.
[18] L. Guo, B. Yan, Eur. J. Inorg. Chem. (2010) 1267–1273.
[19] L.N. Sun, H.J. Zhang, C.Y. Peng, J.B. Yu, Q.G. Meng, L.S. Fu, F.Y. Liu, X.M. Guo, J. Phys. Chem. B 110 (2006) 7249–7258.
[20] Y. Li, B. Yan, H. Yang, J. Phys. Chem. C 112 (2008) 3959–3968.
[21] Y.J. Li, B. Yan, Inorg. Chem. 48 (2009) 8276–8285.
[22] L.L. Kong, B. Yan, Y. Li, J. Alloys Compd. 481 (2010) 549–554.
[23] B. Yan, Y. Li, Dalton Trans. 39 (1480) (2010) 1480–1487.
[24] Y.J. Li, B. Yan, Y. Li, Chem. Asian J. 5 (2010) 1642–1650.
[25] E.M. Hodnett, P.D. Mooney, J. Med. Chem. 13 (1970) 786.
[26] J. Kinski, H. Gies, Zeolites 19 (1995) 375–381.
[27] M.P. Doyle, D.C. Forbes, Chem. Rev. 98 (1998) 911–936.
[28] D. Chandra, T. Yokoi, T. Tatsumi, A. Bhaumik, Chem. Mater. 19 (2007) 5347–5354.
[29] J.L. Liu, S. Xu, B. Yan, Colloids Surf. Sci. A 373 (2011) 116–123.
[30] Y. Li, B. Yan, Solid State Sci. 11 (2009) 994–1000.
[31] Y. Li, B. Yan, J.L. Liu, Nanoscale Res. Lett. 5 (2010) 797–804.
[32] D.D. Perrin, W.L.F. Armarego, D.R. Perrin, Purification of Laboratory Chemicals , Pergamon Press, Oxford, 1980.
[33] D.Y. Zhao, Q.S. Huo, J.L. Feng, B.F. Chmelka, G.D. Stucky, J. Am. Chem. Soc. 120 (1998) 6024–6036.
[34] P.P. Yang, S.S. Huang, D.Y. Kong, J. Lin, H.G. Fu, Inorg. Chem. 46 (2005) 3203–3211.
[35] D.L. Wood, J. Tauc, Phys. Rev. B 5 (1972) 3144–3151.
[36] L.D. Carlos, V.D. Bermudez, R.A.S. Ferreira, L. Marques, M. Assuncao, Chem. Mater. 11 (1999) 581–588.
[37] K.S.W. Sing, D.H. Everett, R.A.W. Haul, L. Moscou, R.A. Pierotti, J. Rouquerol, T. Siemieniewska, Pure Appl. Chem. 57 (1985) 603–619.
[38] M. Kruk, M. Jaroniec, Chem. Mater. 13 (2001) 3169–3183.
[39] C.Y. Peng, H.J. Zhang, Q.G. Meng, H.R. Li, J.B. Yu, F.J. Guo, L.N. Sun, Inorg. Chem. Commun. 8 (2005) 440–442.